Three-Dimensional Analytical Models for Virus Transport in Saturated Porous Media

YOUN SIM and CONSTANTINOS V. CHRYSIKOPOULOS⋆
Department of Civil and Environmental Engineering, University of California, Irvine, CA 92697, U.S.A.

Abstract. Analytical models for virus transport in saturated, homogeneous porous media are developed. The models account for three-dimensional dispersion in a uniform flow field, and first-order inactivation of suspended and deposited viruses with different inactivation rate coefficients. Virus deposition onto solid particles is described by two different processes: nonequilibrium adsorption which is applicable to viruses behaving as solutes; and colloid filtration which is applicable to viruses behaving as colloids. The governing virus transport equations are solved analytically by employing Laplace/Fourier transform techniques. Instantaneous and continuous/periodic virus loadings from a point source are examined.

Nomenclature

a, a_1, a_2	arbitrary constants
$\mathcal{A}$	defined in (9)
A_Ω	amplitude of the virus loading fluctuation, [M/T]
$\mathcal{B}$	defined in (10)
C	concentration of virus in suspension (liquid phase), [M/L^3]
C_0	source concentration, [M/L^3]
C^*	deposited (or filtered) virus concentration (virus mass/solids mass), [M/M]
C_g	concentration of virus directly in contact with solids, [M/L^3]
C_∞	steady state virus concentration in the absence of inactivation, [M/L^3]
D_x	longitudinal hydrodynamic dispersion coefficient, [L^2/T]
D_y	lateral hydrodynamic dispersion coefficient, [L^2/T]
D_z	vertical hydrodynamic dispersion coefficient, [L^2/T]
E	defined in (A7)
f	defined in (A15)
f_0, f_1, f_2	arbitrary functions
F	general functional form of virus source configuration, [M/L^{3}T]
$\mathcal{F}^{-1}$	Fourier inverse operator
g	defined in (A22)
G	virus source loading function, [M/t]
h, h_1, h_2	defined in (A30), (A31) and (A32), respectively
$\mathcal{H}$	defined in (11)
$I_0[\quad]$	modified Bessel function of first kind of order zero

---

⋆ Author to whom correspondence should be addressed.

$I_1[\quad]$	modified Bessel function of first kind of first order
$J_0[\quad]$	Bessel function of first kind of order zero
k	mass transfer rate constant, $[T^{-1}]$
k_c	clogging rate constant, $[T^{-1}]$
k_r	declogging rate constant, $[T^{-1}]$
K_d	partition or distribution coefficient, $[L^3 M^{-1}]$
$K_0[\quad]$	modified Bessel function of second kind of order zero
$l_{x_0}, l_{y_0}, l_{z_0}$	x, y and z Cartesian coordinates, respectively, of the virus point source, [L]
$\mathcal{L}^{-1}$	Laplace inverse operator
M	total virus mass released into the porous formation, [M]
n	wave number
$\mathcal{N}, \mathcal{N}_1, \mathcal{N}_2$	defined in (A24), (A25), and (A26), respectively
p	dummy integration variable
$\mathcal{P}$	defined in (A43)
pfu	plaque-forming units, [M]
q	dummy integration variable
Q	defined in (13)
r_1	forward rate coefficient, $[T^{-1}]$
r_2	reverse rate coefficient, $[M/L^3 T]$
s	Laplace transform variable with respect to time
sse	sums of squared error
$\mathcal{S}$	defined in (A16)
t	time, [T]
t_0	arbitrary time, [T]
t_p	temporal period, [T]
U	average interstitial velocity, [L/T]
v	dummy integration variable
W	virus source geometry function, $[L^{-3}]$
x, y, z	spatial coordinates, [L]

Greek Letters

α	arbitrary constant
α_x	longitudinal dispersivity, [L]
α_y	lateral dispersivity, [L]
α_z	vertical dispersivity, [L]
β	arbitrary constant
γ	Fourier transform variable with respect to spatial coordinate x
$\delta(\ )$	Dirac delta function
ζ	dummy integration variable
η	arbitrary argument
θ	porosity (liquid volume/porous medium volume), $[L^3/L^3]$
λ	inactivation rate coefficient of liquid phase viruses, $[T^{-1}]$
λ^*	inactivation rate coefficient of deposited viruses, $[T^{-1}]$
$\Lambda_1, \Lambda_2, \Lambda_3$	defined in (21a), (21b), and (21c), respectively
ξ	dummy integration variable
ρ	bulk density of the solid matrix (solids mass/aquifer volume), $[M/L^3]$
τ	dummy integration variable
ϕ	Fourier transform variable with respect to spatial coordinate z
Φ	defined in (A18)
Ψ	defined in (A13)
ω	Fourier transform variable with respect to spatial coordinate y
Ω_n	spectrum of known coefficients, [M/T]
$\overline{\Omega}$	mean virus mass release rate, [M/T]

1. Introduction

Groundwater contamination by pathogenic viruses is a significant environmental concern throughout the world. The penetration of viruses into aquifers is often associated with pollution sources such as direct injection into wells, recharge basins, irrigation, landfills, open dumps, graveyards, broken sewer pipelines, leaking septic tanks, and urban runoff (Keswick and Gerba, 1980; Armon and Kott, 1994; Zelikson, 1994). It should be noted that although sludges are treated by various disinfection methods such as chlorination and heat conditioning prior to disposal, highly resistant viruses may remain infective (Berg, 1977).

Viruses are colloid particles with size ranging from 0.02 to 0.3 μm (Brock and Madigan, 1991). They vary widely in shape and chemical composition. Their surface charge is established by the ionizable groups comprising the virus surface (capsid); furthermore, at natural subsurface conditions viruses are generally negatively charged (Taylor and Bosmann, 1981; Elimelech *et al.*, 1995). Because viruses do not have their own respiratory and biosynthetic functions, they reproduce inside other cells by a process called infection. Therefore, unlike bacteria or protozoa, viruses present in groundwater can not increase in numbers, but only decrease. Viruses are classified on the basis of the hosts they infect. The most common types of viruses found in groundwater which may infect human body are animal viruses such as: *adenovirus, coliphage, coxsackievirus, enterovirus, hepatitis, poliovirus* and *rotavirus* (Gerba and Keswick, 1981; Yates and Yates, 1988). As illustrated in Figure 1, viruses are larger than dissolved contaminants, however, it should be noted that viruses are at the lower end of the colloid size distribution. For this reason, virus adsorption onto the solid matrix of a subsurface formation is described by either colloid filtration or solute sorption processes.

Vilker (1981) suggested that the nonequilibrium adsorption process is appropriate for models describing virus transport in porous media, assuming viruses behave as solutes. Nonequilibrium adsorption represents the rate of approach to equilibrium between adsorbed and liquid phase virus concentrations, accounting for virus transport to the outer layer of a solid particle by mass transfer followed by virus immobilization. The colloid filtration theory is frequently employed to models of virus transport in porous media, assuming viruses behave as colloids. Colloids are attached onto the solid matrix through interception, sedimentation (mechanical filtration), and diffusion. The interception and sedimentation processes are effective only for large size particles ($\geqslant 1$ μm). Because viruses are of submicron size (see Figure 1), for the case of virus filtration, the effects of sedimentation and interception can be neglected (Harvey and Garabedian, 1991; Penrod, 1995).

There are only a few analytical (Vilker *et al.*, 1978; Sim and Chrysikopoulos, 1995; Chrysikopoulos and Sim, 1996) and numerical (Grosser, 1984; Haridas, 1984; Tim and Mostaghimi, 1991; Park *et al.*, 1992; Yates and Ouyang, 1992; Sim and Chrysikopoulos, 1996a) models available in the literature for the prediction of fate and transport of viruses in subsurface formations. Analytical virus transport models,
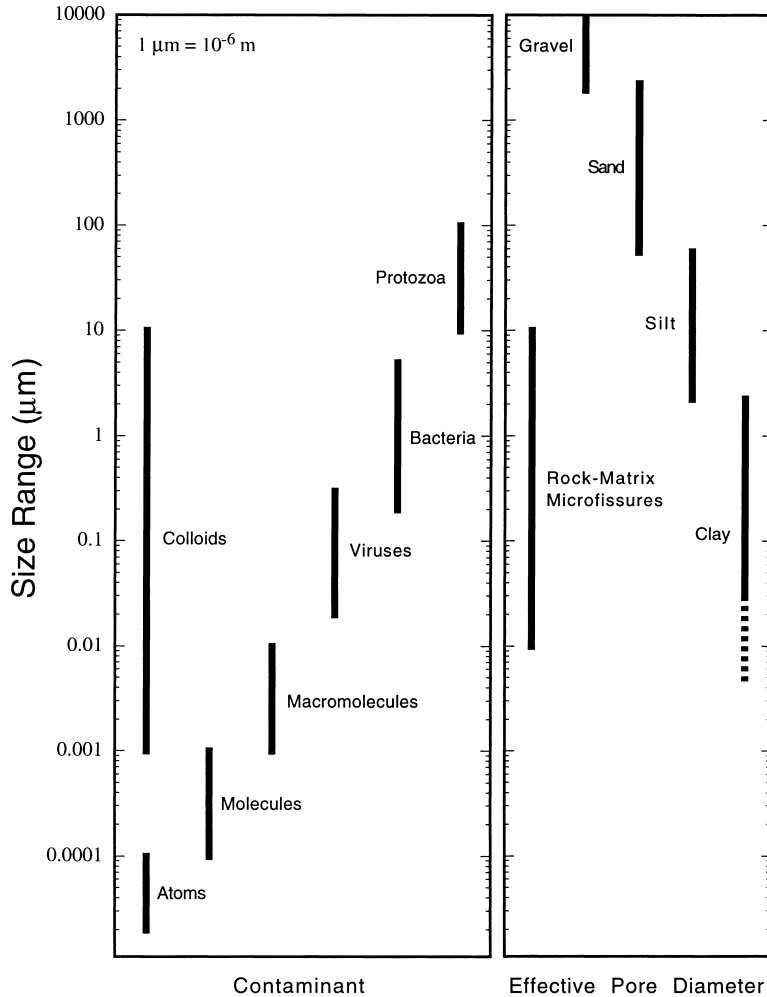
Figure 1. Size ranges of contaminants present in groundwater and effective pore diameters of various porous media, adopted from Chrysikopoulos and Sim (1996). Contaminant sizes are obtained from Stumm (1977), Matthess and Pekdeger (1981), and Buddemeier and Hunt (1988); microfissure sizes are obtained from Birgersson and Neretnieks (1982); effective pore diameters are calculated from average soil particle diameters reported by Mitchell (1976), by assuming a cubic packing: effective pore diameter = particle diameter $\times \sqrt{2} - 1$).

although limited by many assumptions, are very useful tools for preliminary estimation of virus migration, examination of possible boundary conditions, validation of numerical solutions, and determination of virus transport parameters from laboratory or well defined field experiments.

Multidimensional contaminant transport models have several advantages over one-dimensional models. For example, multidimensional models can account for concentration gradients and contaminant transport in directions perpenticular to the

groundwater flow. As indicated by Leij and Dane (1990), measuring experimentally lateral and vertical dispersion coefficients is not a trivial task. However, multidimensional transport models can provide such parameters by direct fitting of available experimental data. In addition, multidimensional models can easily account for a variety of boundary conditions as well as contaminant source geometries.

Although several multidimensional, analytical solute transport models have been presented in the literature (Hunt, 1978; Goltz and Roberts, 1986; van Dujin and van der Zee, 1986; Batu, 1989, 1993; Batu and van Genuchten, 1990; Leij and Dane, 1990; Leij *et al.*, 1991, 1993; Bellin *et al.*, 1993; Chrysikopoulos *et al.*, 1994; Chrysikopoulos, 1995; to mention a few), to our knowledge, the literature on multidimensional analytical virus transport models is nonexistent. Consequently, the present research focuses on the development of analytical solutions for three-dimensional models of virus transport in porous media. Generalized analytical solutions applicable to nonequilibrium virus deposition and filtration under instantaneous, continuous and temporally fluctuating point source virus loading conditions are derived.

2. Model Development

The transport of viruses in saturated, homogeneous porous media, accounting for three-dimensional hydrodynamic dispersion in a uniform flow field, virus adsorption, and first-order inactivation of liquid phase and deposited viruses with different inactivation rate coefficients, is governed by the following partial differential equation

$$\frac{\partial C(t, x, y, z)}{\partial t} +$$

$$+\frac{\rho}{\theta}\frac{\partial C^*(t, x, y, z)}{\partial t} - D_x\frac{\partial^2 C(t, x, y, z)}{\partial x^2} -$$

$$-D_y\frac{\partial^2 C(t, x, y, z)}{\partial y^2} - D_z\frac{\partial^2 C(t, x, y, z)}{\partial z^2} + U\frac{\partial C(t, x, y, z)}{\partial x} +$$

$$+\lambda C(t, x, y, z) + \lambda^*\frac{\rho}{\theta}C^*(t, x, y, z) = F(t, x, y, z), \tag{1}$$

where C is the liquid phase virus concentration; C^* is the virus concentration deposited onto the solid matrix; D_x, D_y, and D_z are the longitudinal, lateral, and vertical hydrodynamic dispersion coefficients, respectively; U is the average interstitial velocity; t is time; x, y, and z are the spatial coordinates in the longitudinal, lateral, and vertical directions, respectively; ρ is the bulk density of the solid matrix; θ is the porosity of the porous medium; λ is the inactivation rate coefficient of liquid phase viruses; λ^* is the inactivation rate coefficient of deposited viruses; and F is a general form of the virus source configuration. The first two terms on the left-hand side of the preceding equation are accumulation terms, whereas the last two terms on the left-hand side represent the inactivation of liquid phase and deposited viruses,

respectively. The accumulation of deposited viruses on the solid matrix is described by the following generalized mass balance expression

$$\frac{\rho}{\theta} \frac{\partial C^*(t, x, y, z)}{\partial t}$$
$$= r_1 C(t, x, y, z) - r_2 C^*(t, x, y, z) - \lambda^* \frac{\rho}{\theta} C^*(t, x, y, z), \tag{2}$$

where r_1 and r_2 are the forward and the reverse rate coefficients. The appropriate initial and boundary conditions for an infinite three-dimensional porous medium are

$$C(0, x, y, z) = C^*(0, x, y, z) = 0, \tag{3}$$

$$C(t, \pm\infty, y, z) = 0, \tag{4}$$

$$C(t, x, \pm\infty, z) = 0, \tag{5}$$

$$C(t, x, y, \pm\infty) = 0. \tag{6}$$

The expression describing C^* is obtained by solving (2) subject to the initial condition (3) to yield

$$C^*(t, x, y, z) = \frac{r_1 \theta}{\rho} \int_0^t C(\tau, x, y, z) \exp\left[-\left(\frac{r_2 \theta}{\rho} + \lambda^*\right)(t - \tau)\right] d\tau, \tag{7}$$

where τ is a dummy integration variable. In view of (2) and (7) the governing equation (1) can be written as

$$\frac{\partial C(t, x, y, z)}{\partial t} -$$

$$- D_x \frac{\partial^2 C(t, x, y, z)}{\partial x^2} - D_y \frac{\partial^2 C(t, x, y, z)}{\partial y^2} - D_z \frac{\partial^2 C(t, x, y, z)}{\partial z^2} +$$

$$+ U \frac{\partial C(t, x, y, z)}{\partial x} + \mathcal{A} C(t, x, y, z) -$$

$$- \mathcal{B} \int_0^t C(\tau, x, y, z) e^{-\mathcal{H}(t-\tau)} d\tau = F(t, x, y, z), \tag{8}$$

where the following substitutions have been employed

$$\mathcal{A} = r_1 + \lambda, \tag{9}$$

$$\mathcal{B} = \frac{r_1 r_2 \theta}{\rho}, \tag{10}$$

$$\mathcal{H} = \frac{r_2 \theta}{\rho} + \lambda^*. \tag{11}$$

Equation (8) subject to conditions (3)–(6) is solved analytically by straightforward but laborious procedures. Taking Laplace transforms with respect to time variable t and Fourier transforms with respect to space variables x, y, and z of (8) and subsequently employing the transformed initial and boundary conditions, followed by inverse transformations yields the desired analytical solution (see Appendix A)

$$C(t, x, y, z) = \left(\frac{1}{16\pi^2 D_x D_y} \right)^{1/2} \int_0^t \int_{-\infty}^\infty \int_{-\infty}^\infty \int_{-\infty}^\infty \times$$

$$\times \exp\left[\frac{U(x - q)}{2D_x} \right] F(t - \tau, q, v, p) \times$$

$$\times \left[\mathcal{H} Q(\tau, x - q, y - v, z - p) + \right.$$

$$\left. + \frac{\partial Q(\tau, x - q, y - v, z - p)}{\partial \tau} \right] dp \, dv \, dq \, d\tau, \qquad (12)$$

where

$$Q(t, x, y, z) = e^{-\mathcal{H}t} \int_0^t I_0 \left[2(\mathcal{B}\zeta(t - \zeta))^{1/2} \right] \left(\frac{1}{4\pi D_z \zeta^3} \right)^{1/2} \times$$

$$\times \exp\left[-\frac{1}{4\zeta} \left(\frac{x^2}{D_x} + \frac{y^2}{D_y} + \frac{z^2}{D_z} \right) - \right.$$

$$\left. - \zeta \left(\mathcal{A} + \frac{U^2}{4D_x} - \mathcal{H} \right) \right] d\zeta, \qquad (13)$$

$$\frac{\partial Q(t, x, y, z)}{\partial t}$$

$$= e^{-\mathcal{H}t} \int_0^t \left\{ \left(\frac{\mathcal{B}\zeta}{t - \zeta} \right)^{1/2} I_1 \left[2(\mathcal{B}\zeta(t - \zeta))^{1/2} \right] - \right.$$

$$\left. - \mathcal{H} I_0 \left[2(\mathcal{B}\zeta(t - \zeta))^{1/2} \right] \right\} \left(\frac{1}{4\pi D_z \zeta^3} \right)^{1/2} \times$$

$$\times \exp\left[-\frac{1}{4\zeta} \left(\frac{x^2}{D_x} + \frac{y^2}{D_y} + \frac{z^2}{D_z} \right) - \zeta \left(\mathcal{A} + \frac{U^2}{4D_x} - \mathcal{H} \right) \right] d\zeta +$$

$$+ e^{-\mathcal{H}t} \left(\frac{1}{4\pi D_z t^3} \right)^{1/2} \exp\left[-\frac{1}{4t} \left(\frac{x^2}{D_x} + \frac{y^2}{D_y} + \frac{z^2}{D_z} \right) - \right.$$

$$\left. - t \left(\mathcal{A} + \frac{U^2}{4D_x} - \mathcal{H} \right) \right], \qquad (14)$$

where I_0 and I_1 are the modified Bessel functions of the first kind of zeroth and first order, respectively. It should be noted that the Leibnitz rule (Greenberg, 1978, eq. 1.41, p. 18) as well as the Bessel function relationships $dI_0[\eta]/d\eta = I_1[\eta]$ (Abramowitz and Stegun, 1972, Equation 9.6.27, p. 376) and $I_0[0] = 1$ were employed in the derivation of (14).

2.1. POINT SOURCE CONFIGURATION

The virus source configuration is represented by the following general function

$$F(t, x, y, z) = G(t)W(x, y, z), \tag{15}$$

where $G(t)$ is the virus mass release rate from the source; and $W(x, y, z)$ signifies the inverse of the source volume from which the virus mass is introduced into a porous medium. It should be noted, however, that $G(t)$ characterizes the source loading type. In this work, instantaneous as well as continuous or temporally periodic source loading functions are considered. Furthermore, $W(x, y, z)$ characterizes the source physical geometry. Although point, two and three-dimensional source geometries can be applied to the general analytical solution derived (12)–(14), the present research efforts focus on a point source configuration as illustrated schematically in Figure 2, which can be described mathematically by

$$W(x, y, z)$$

$$= \frac{1}{\theta}\delta(x - l_{x_0})\delta(y - l_{y_0})\delta(z - l_{z_0}), \quad -\infty < l_{x_0}, l_{y_0}, l_{z_0} < \infty, \tag{16}$$

where $l_{x_0}, l_{y_0}, l_{z_0}$ represent x, y, z Cartesian coordinates of the virus point source, respectively; and δ is the Dirac delta function.

2.1.1. *Instantaneous Virus Loading*

For the case of instantaneous virus loading, the mass release rate function is described by the following expression

$$G(t) = M\delta(t - t_0), \tag{17}$$

where M signifies the total virus mass released; and t_0 is the time of instantaneous virus release. Combining (12) and (15)–(17) yields

$$
\begin{aligned}
C(t, x, y, z) = \ &\frac{M}{\theta}\left(\frac{1}{16\pi^2 D_x D_y}\right)^{1/2}\exp\left[\frac{U(x - l_{x_0})}{2D_x}\right] \times \\
&\times \left[\ \mathcal{H}Q(t - t_0, x - l_{x_0}, y - l_{y_0}, z - l_{z_0}) + \right.\\
&\left. +\frac{\partial Q(t - t_0, x - l_{x_0}, y - l_{y_0}, z - l_{z_0})}{\partial t}\right],
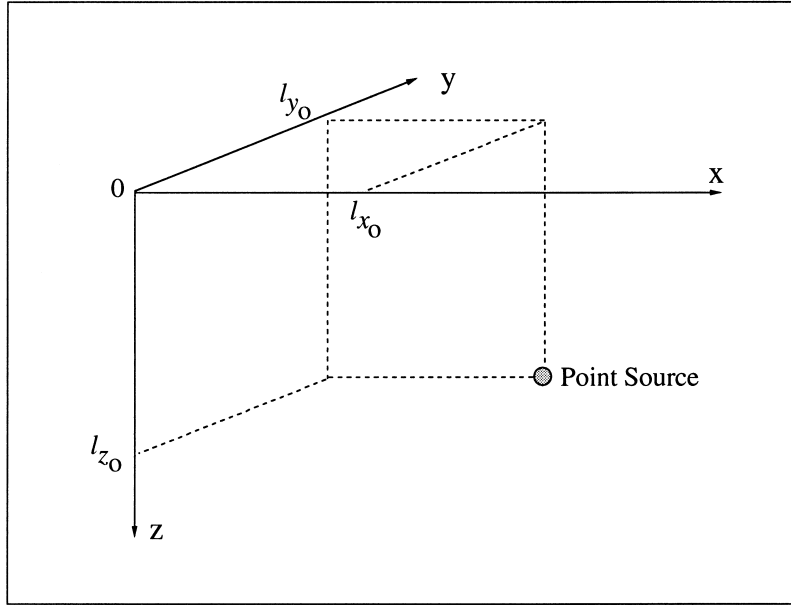\end{aligned}
\tag{18}
$$

Figure 2. Schematic illustration of a virus point source with coordinates $l_{x_0}, l_{y_0}, l_{z_0}$.

where the following property of Dirac delta function was employed

$$\int_{\alpha}^{\beta} f_0(t)\delta(t - t_0)\, dt = f_0(t_0), \quad \alpha \leqslant t_0 \leqslant \beta, \tag{19}$$

and f_0 is an arbitrary function. The desired analytical solution for the case of instantaneous virus loading conditions is obtained by substituting (13) and (14) into (18), to yield

$$C(t, x, y, z)$$

$$= \frac{M}{\theta} \int_0^{t-t_0} \left(\frac{1}{64\pi^3 D_x D_y D_z \zeta^3} \right)^{1/2} \times$$

$$\times \Lambda_1(t - t_0)\, \Lambda_2(t - t_0)\, \Lambda_3(\zeta, x - l_{x_0}, y - l_{y_0}, z - l_{z_0})\, d\zeta \; +$$

$$+ \frac{M}{\theta} \left(\frac{1}{64\pi^3 D_x D_y D_z (t - t_0)^3} \right)^{1/2} \times$$

$$\times \Lambda_1(t - t_0)\, \Lambda_3(t - t_0, x - l_{x_0}, y - l_{y_0}, z - l_{z_0}), \tag{20}$$

where the following definitions were employed

$$\Lambda_1(t) = \exp\left[-\mathcal{H}t \right], \tag{21a}$$

$$\Lambda_2(t) = \left(\frac{\mathcal{B}\zeta}{t - \zeta} \right)^{1/2} I_1\left[2(\mathcal{B}\zeta(t - \zeta))^{1/2} \right], \tag{21b}$$

$$\Lambda_3(t, x, y, z) = \exp\left[\frac{Ux}{2D_x} - \frac{1}{4t}\left(\frac{x^2}{D_x} + \frac{y^2}{D_y} + \frac{z^2}{D_z}\right) - \right.$$

$$\left. -t\left(\mathcal{A} + \frac{U^2}{4D_x} - \mathcal{H}\right)\right], \tag{21c}$$

and ζ is a dummy integration variable.

2.1.2. *Continuous or Periodic Virus Loading*

For the case of a continuous or temporally periodic virus loading, the mass release rate function can be represented by a generalized Fourier series (Hassani, 1991)

$$G(t) = \overline{\Omega} + \sum_{n=1}^{\infty} \Omega_n \exp\left[\frac{i2n\pi t}{t_p}\right], \tag{22}$$

where $\overline{\Omega}$ represents the mean value of the virus mass release rate from the source; Ω_n is a spectrum of known coefficients; n is the wave number; and t_p is the temporal period of fluctuation. It should be noted that for the special case of an infinite period $(t_p \rightarrow \infty)$, (22) reduces to a constant rate source loading ($G = \overline{\Omega}$). In view of (19), combining (12) with (15), (16) and (22) yields

$$C(t, x, y, z) = \left(\frac{1}{16\pi^2 D_x D_y}\right)^{1/2} \int_0^t \times$$

$$\times \exp\left[\frac{U(x - l_{x_0})}{2D_x}\right]\frac{G(t - \tau)}{\theta} \times$$

$$\times\left[\ \mathcal{H}Q(\tau, x - l_{x_0}, y - l_{y_0}, z - l_{z_0}) + \right.$$

$$\left. + \frac{\partial Q(\tau, x - l_{x_0}, y - l_{y_0}, z - l_{z_0})}{\partial \tau}\right]d\tau. \tag{23}$$

The desired analytical solution for continuous/periodic virus loading conditions is obtained by substituting (13) and (14) into (23), to yield

$$C(t, x, y, z) = \int_0^t \int_0^\tau \left(\frac{1}{64\pi^3 D_x D_y D_z \zeta^3}\right)^{1/2} \frac{G(t - \tau)}{\theta} \times$$

$$\times \Lambda_1(\tau)\,\Lambda_2(\tau)\,\Lambda_3(\zeta, x - l_{x_0}, y - l_{y_0}, z - l_{z_0})\,d\zeta\,d\tau + $$

$$+ \int_0^t \left(\frac{1}{64\pi^3 D_x D_y D_z \tau^3}\right)^{1/2} \frac{G(t - \tau)}{\theta} \times$$

$$\times \Lambda_1(\tau)\,\Lambda_3(\tau, x - l_{x_0}, y - l_{y_0}, z - l_{z_0})\,d\tau. \tag{24}$$

2.2. NONEQUILIBRIUM VIRUS ADSORPTION (S MODEL)

Assuming that the adsorption process consists of virus diffusion to the outer layer of a solid particle by nonequilibrium mass transfer and virus immobilization onto the solid particle while in equilibrium with the liquid phase virus concentration in the outer layer, the expression for accumulation of adsorbed viruses (2) can be replaced by (Sim and Chrysikopoulos, 1996a)

$$\frac{\rho}{\theta}\frac{\partial C^*(t, x, y, z)}{\partial t} = k\Big[C(t, x, y, z) - C_g(t, x, y, z)\Big] - \lambda^*\frac{\rho}{\theta}C^*(t, x, y, z), \qquad (25)$$

where k is the mass transfer rate constant; and C_g is the liquid phase concentration of virus in direct contact with solids. Vilker (1981) suggested that the Langmuir isotherm may represent the equilibrium relationship between immobilized viruses and viruses in the outer layer of the solid matrix. However, experimental results indicated that for low liquid phase virus concentrations and when conditions are such that virus affinity for the adsorbent is very small, the nonlinear form of the Langmuir isotherm can be linearized to the following linear equilibrium relationship

$$C^*(t, x, y, z) = K_d C_g(t, x, y, z), \qquad (26)$$

where K_d is the partition or distribution coefficient. The nonequilibrium adsorption model is appropriate for viruses with size relatively small or similar to the size of solutes. Thus, molecular diffusion together with local hydrodynamic conditions control the adsorption of viruses onto the solid matrix.

In view of (2), (25), and (26), the following substitutions

$$r_1 = k, \qquad (27)$$

$$r_2 = \frac{k}{K_d}, \qquad (28)$$

can be employed into (20) or (24) to yield the corresponding S model solution for either instantaneous or continuous virus loading, respectively.

2.3. VIRUS FILTRATION (C MODEL)

Assuming that the colloid filtration theory is applicable to virus attachment onto the solid matrix of a subsurface formation, the accumulation of filtered viruses can be written as

$$\frac{\rho}{\theta}\frac{\partial C^*(t, x, y, z)}{\partial t}$$

$$= k_c C(t, x, y, z) - k_r \frac{\rho}{\theta}C^*(t, x, y, z) - \lambda^*\frac{\rho}{\theta}C^*(t, x, y, z), \qquad (29)$$

where C^* is now the virus concentration retained in the porous medium by the filtration process; k_c is the clogging rate constant; and k_r is the declogging rate constant.

For viruses with size considerably larger than the size of solutes, the filtration model can represent the attachment of viruses onto the solid matrix more appropriately by incorporating the effect of virus size, solid size, and interstitial water velocity.

In view of (2) and (29) the following substitutions

$$r_1 = k_c, \tag{30}$$

$$r_2 = \frac{k_r \rho}{\theta}, \tag{31}$$

can be employed into (20) or (24) to yield the corresponding C model solution for either instantaneous or continuous virus loading, respectively.

3. Model Simulations and Discussion

Model simulations under nonequilibrium virus adsorption (S model) as well as virus filtration (C model) conditions and two different source configurations are performed for a variety of situations. The integrals present in the analytical solutions (20) and (24) are evaluated numerically by the integration routine Q1DA, which utilizes an automatic adaptive quadrature algorithm (Kahaner *et al.*, 1989). The virus source is assumed to be located at $l_{x_0} = l_{y_0} = l_{z_0} = 100$ cm, and the instantaneous virus release to occur at $t_0 = 0$ d. For simplicity, the values for M and $\overline{\Omega}$ are set to unity. Unless otherwise specified, the fixed parameter values used in the simulations are those listed in Table I. Furthermore, the concentrations generated under continuous virus loading conditions are normalized by the steady-state concentration in the absence of inactivation, evaluated at $t = 100$ d (C_∞) as suggested by Hunt (1978).

The solution to the C model under continuous virus loading conditions (Equations (24), (30), (31)) is employed to investigate the effect of the two different inactivation rate coefficients incorporated into the governing virus transport equation (1) on suspended virus concentration. Figures 3a and 3b present breakthrough curves at a location with coordinates $x = 109$ cm and $y = z = 100$ cm, for three different inactivation rate coefficients for liquid phase (λ) and adsorbed (λ^*) viruses, respectively. Concentration profiles are conveniently normalized by the steady-state concentration in the absence of inactivation. It is shown that the liquid phase virus

Table I. Model parameters for simulations.

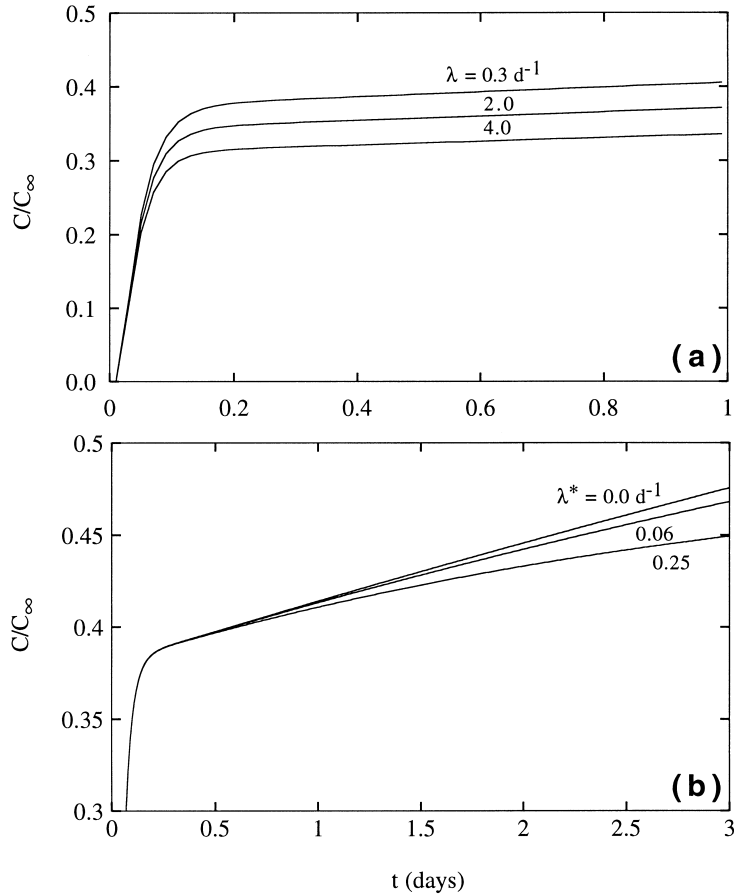| Parameter	Value
D_x	15 cm^2/hr
$D_y = D_z$	1.13 cm^2/hr
K_d	20 ml/g
U	4 cm/hr
ρ	1.5 g/cm^3
θ	0.25

Figure 3. Effect of the inactivation rate coefficients for (a) liquid phase and (b) adsorbed viruses on temporal normalized virus distribution simulated by the C model under continuous virus loading conditions. (Here $x = 109$ cm, $y = z = 100$ cm, $k_c = 0.6$ hr^{-1}, $k_r = 0.005$ hr^{-1}, $\lambda = 0.25$ d^{-1}, and $\lambda^* = 0$ d^{-1}.)

concentration decreases with increasing λ and λ^*. This result is intuitive because an increase in λ or λ^* implies an increase in the inactivation rate of liquid phase or adsorbed viruses, respectively, and consequently a decrease in the concentration of suspended viruses.

Two-dimensional snapshots of virus concentration simulated by the C model under instantaneous virus loading conditions (Equations (20), (30), (31)) at three successive times are illustrated in Figure 4. As the center of mass moves downstream from the source, enhanced spreading is observed in both longitudinal and lateral directions. However, it is observed that the migration of the virus plume is significantly retarded and an elongated tail of viruses is trailing behind the center of mass. This result is consistent with field observations of virus transport where virus
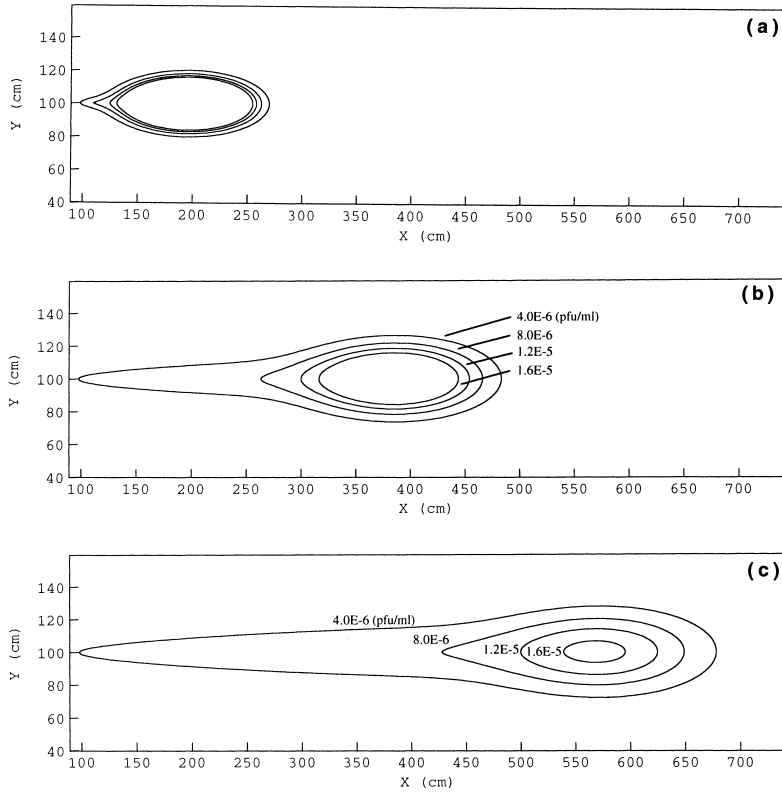
Figure 4. Concentration contours in the x, y plane obtained by the C model under instantaneous loading of viruses undergoing reversible deposition at (a) $t = 1.0$ d, (b) $t = 3.0$ d, and (c) $t = 5.0$ d. (Here $z = 100$ cm, $k_c = 0.001$ hr^{-1}, $k_r = 0.1$ hr^{-1}, and $\lambda = \lambda^* = 0$ d^{-1}.)

plumes undergoing reversible deposition were considerably retarded compared to a conservative tracer (Bales *et al.*, 1995).

The general behavior of the S model is similar to the C model. For example, Figure 5 illustrates two-dimensional snapshots of virus concentrations on the x, y plane, at three successive times as predicted by the S model under continuous but constant ($G = \overline{\Omega}$) virus loading conditions (Equations (24), (27), (28)). For the case examined here, the virus loading is continuous as opposed to instantaneous loading considered in Figure 4.

The effect of periodic source loading conditions on the temporal distribution of virus concentration is illustrated in Figure 6. Breakthrough curves at three different locations along the x–axis downstream from the source with fixed coordinates $y = z = 100$ cm are simulated by the S model (Equations (24), (27), (28)) under continuous virus loading from a temporally variable source (dashed curves) and from a constant source ($G = \overline{\Omega}$, solid curves). In the interest of computational simplicity,
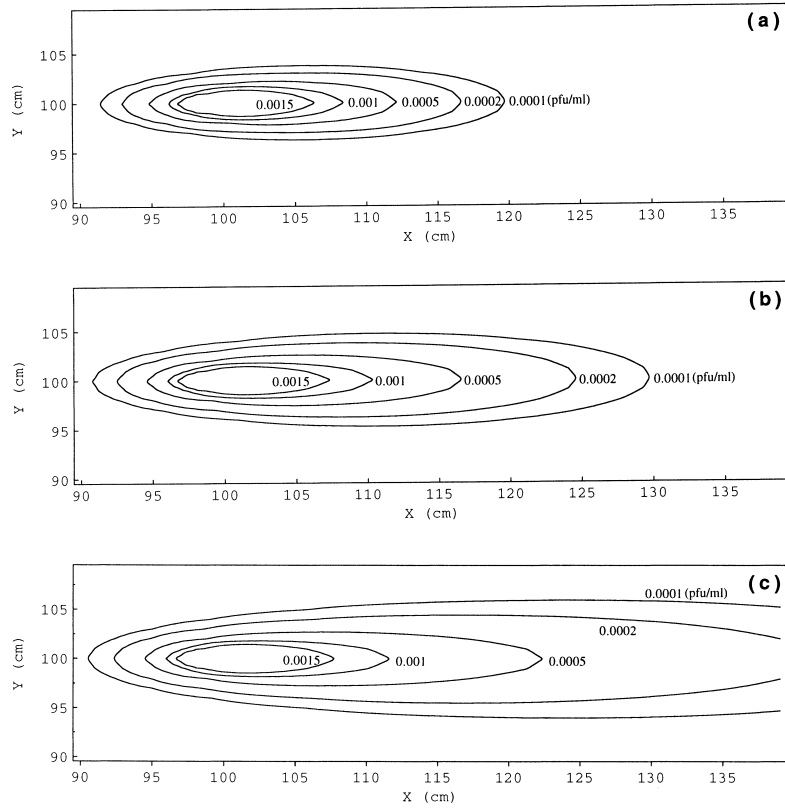
Figure 5. Concentration contours in the x, y plane obtained by the S model under continuous virus loading conditions at (a) $t = 0.1$ d, (b) $t = 0.2$ d, and (c) $t = 0.5$ d. (Here $z = 100$ cm, $k = 0.0001$ hr^{-1}, and $\lambda = \lambda^* = 0$ d^{-1}.)
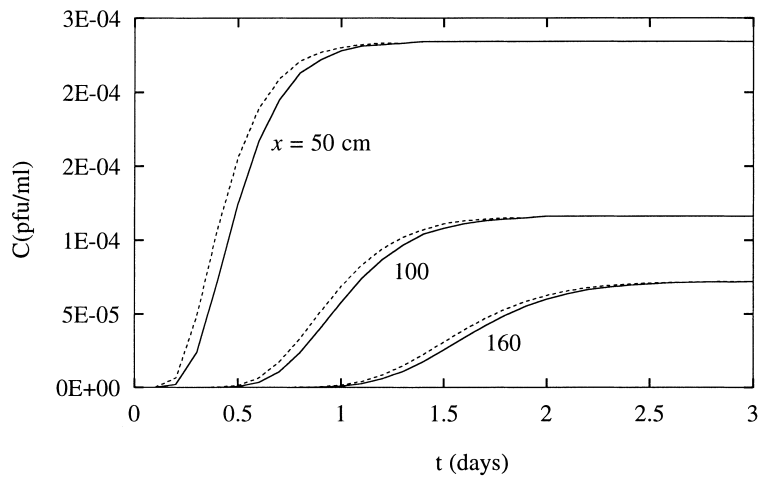

Figure 6. Breakthrough curves predicted by the S model under periodic (dashed curves) and constant (solid curves) loading conditions. (Here $y = z = 100$ cm, $A_\Omega = 1$ pfu/d, $t_p = 0.08$ d, $k = 0.0001$ hr^{-1}, and $\lambda = \lambda^* = 0$ d^{-1}.)

the generalized expression for a temporally variable source loading rate (22) is modified as

$$G(t) = \overline{\Omega} + A_\Omega \sin\left[\frac{2\pi t}{t_p}\right], \tag{32}$$

where A_Ω represents the amplitude of the virus loading fluctuation. It is evident from Figure 6 that the difference between the virus breakthrough responses simulated under periodic and constant source loading rates is significant in the vicinity of the source and gradually diminishes with increasing distance from the source. Therefore, at a relatively long distance downstream from a source, the effect of temporally variable source loading on the concentration of suspended viruses is negligible. This is in agreement with previous parameter sensitivity analysis results indicating that at large time, model parameter fluctuations have insignificant effects on virus transport (Sim and Chrysikopoulos, 1996b).

4. Comparison with Experimental Data

The analytical solution derived for a point source geometry under instantaneous loading conditions (Equation (20)) is employed to simulate data from a bacterio-phage PRD–1 transport experiment in a sandy aquifer in Borden, Ontario, Canada, reported by Bales *et al.* (1997). Bacteriophage PRD–1 is a virus that infects only certain strains of *Salmonella* bacteria. The field experiment was conducted with a point source geometry under instantaneous loading conditions. The field data used in this study were collected at monitoring well ML4–6. For simplicity, it is assumed that $\alpha_x/10 = \alpha_y = \alpha_z$, where α_x, α_y, and α_z are the longitudinal, lateral, and vertical dispersivities, respectively ($D_i = \alpha_i U$, $i = x, y, z$). Given the experimental parameters M, U, θ, λ, λ^*, and ρ listed in Table II, the values for r_1, r_2, and α_x are estimated by a nonlinear least squares regression method (IMSL, 1991). The estimated parameter values together with the corresponding residual sums of squared error (sse) are presented in Table II. Figure 7 clearly shows a good agreement between the simulated concentration history (solid line) and the bacteriophage PRD–1 experimental data (circles). In view of the estimated values for r_1 and r_2, the corresponding nonequilibrium sorption parameters k and K_d are calculated from (27), (28), whereas the filtration parameters k_c and k_r are calculated from (30), (31) and they are also listed in Table II. It should be noted that the estimated longitudinal dispersivity at ML4–6 ($\alpha_x = 27.36$ cm) is within the range of values (10–60 cm) obtained by Li (1993) from electrical conductivity breakthrough curves.

5. Summary and Conclusions

Analytical models for virus transport in saturated, homogeneous porous media were developed, accounting for three-dimensional hydrodynamic dispersion in a uniform flow field, first-order inactivation of liquid phase and deposited viruses with different inactivation rate coefficients, and virus attachment onto the solid matrix

Table II. Parameters associated with the bacteriophage PRD–1 field experiment.

Experimental parameters (Bales *et al.*, 1997)	
M	1.24×10^{13} pfu
t_0	0 d
U	9 cm/d
x	100.0 cm
θ	0.3
$\lambda = \lambda^*$	0 d^{-1}
ρ	1.81 g/cm^3
Estimated parameters	
r_1	0.21 hr^{-1}
r_2	0.0046 g/cm^3 hr
α_x	27.36 cm
sse	8.76
Calculated parameters	
k	0.21 hr^{-1}
K_d	46.19 cm^3/g
k_c	0.21 hr^{-1}
k_r	0.0008 hr^{-1}
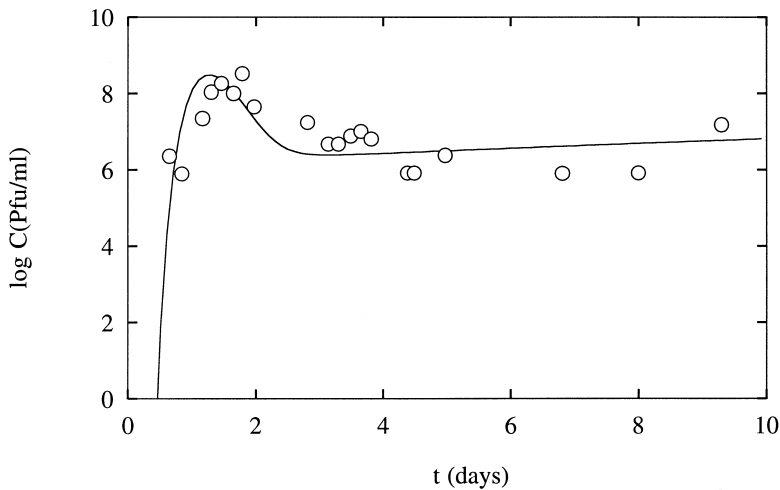
Figure 7. Bacteriophage PRD-1 normalized concentration breakthrough data (open circles) adopted from Bales *et al.* (1997) and simulated concentration history (solid curve).

of the porous formation by either nonequilibrium adsorption (S model) or modified colloid filtration (C model). The governing transport equations were solved analytically by employing Laplace/Fourier transform techniques. A point source geometry was examined under instantaneous as well as continuous/periodic loading

conditions. Results from numerous model simulations indicate that the suspended virus migration in the subsurface is significantly controlled by virus attachment onto solid matrix, and the inactivation of liquid phase as well as deposited viruses. The effect of temporally variable virus loading, as compared to the case of constant rate loading, is maximum near the source and diminishes with increasing distance from the source. Therefore, virus concentration predictions corresponding to temporally variable and constant rate sources are indistinguishable at relatively distant downstream locations from the source.

Although the models presented here have advantages due to their analytical nature, some of the limitations inherent to the models are their inability to account for (a) aquifer heterogeneities; and (b) time-dependent inactivation rate coefficients. Nonetheless, these models are excellent means for verifying the accuracy of numerical approximations to more comprehensive models for virus transport in the subsurface.

Appendix A: Derivation of the Generalized Analytical Solution

The desired analytical solution is obtained by solving the problem described by the following integrodifferential equation and initial/boundary conditions

$$\frac{\partial C(t, x, y, z)}{\partial t} -$$

$$-D_x \frac{\partial^2 C(t, x, y, z)}{\partial x^2} - D_y \frac{\partial^2 C(t, x, y, z)}{\partial y^2} -$$

$$-D_z \frac{\partial^2 C(t, x, y, z)}{\partial z^2} + U \frac{\partial C(t, x, y, z)}{\partial x} + \mathcal{A} C(t, x, y, z) -$$

$$-\mathcal{B} \int_0^t C(\tau, x, y, z) e^{-\mathcal{H}(t-\tau)} \, d\tau = F(t, x, y, z), \tag{A1}$$

$$C(0, x, y, z) = 0, \tag{A2}$$

$$C(t, \pm\infty, y, z) = 0, \tag{A3}$$

$$C(t, x, \pm\infty, z) = 0, \tag{A4}$$

$$C(t, x, y, \pm\infty) = 0. \tag{A5}$$

Taking Laplace transform with respect to time variable t and Fourier transforms with respect to space variables x, y, and z of Equation (A1) and subsequently employing transformed initial condition (A2) yields

$$\dot{\bar{\bar{\bar{C}}}}(s, \gamma, \omega, \phi) = \frac{\dot{\bar{\bar{\bar{F}}}}(s, \gamma, \omega, \phi)}{\gamma^2 D_x + i\gamma U + E}, \tag{A6}$$

where

$$E = \omega^2 D_y + \phi^2 D_z + \mathcal{A} + s - \frac{\mathcal{B}}{s + \mathcal{H}}, \tag{A7}$$

and the following properties were employed for the Laplace and Fourier transformations (Roberts and Kaufman, 1966; Kreyszig, 1993)

$$\dot{\overline{\hat{\tilde{C}}}}(s, \gamma, \omega, \phi) = \frac{1}{(2\pi)^{3/2}} \int_{-\infty}^{\infty} \int_{-\infty}^{\infty} \int_{-\infty}^{\infty} \int_{0}^{\infty} C(t, x, y, z) \times$$

$$\times \mathrm{e}^{-st} \, \mathrm{e}^{-i\gamma x} \, \mathrm{e}^{-i\omega y} \, \mathrm{e}^{-i\phi z} \, \mathrm{d}t \, \mathrm{d}x \, \mathrm{d}y \, \mathrm{d}z, \tag{A8}$$

where the tilde signifies Laplace transform and s is the Laplace domain variable; the hat, overbar, and overdot signify Fourier transforms with respect to space variables x, y, and z with corresponding Fourier domain variables γ, ω, and ϕ, respectively; and $i = (-1)^{1/2}$.

The Fourier inverse transformation of (A6) with respect to γ is

$$\dot{\overline{\tilde{C}}}(s, x, \omega, \phi)$$

$$= \frac{\dot{\overline{\tilde{F}}}(s, x, \omega, \phi)}{2\pi D_x} \, *$$

$$* \left(\int_{-\infty}^{\infty} \frac{\cos \gamma x}{\gamma^2 + \frac{i\gamma U}{D_x} + \frac{E}{D_x}} \, \mathrm{d}\gamma + \int_{-\infty}^{\infty} \frac{i \sin \gamma x}{\gamma^2 + \frac{i\gamma U}{D_x} + \frac{E}{D_x}} \, \mathrm{d}\gamma \right), \tag{A9}$$

where $\mathcal{F}^{-1}$ is the Fourier inverse operator; the asterisk represents convolution with respect to space variable x; and the following definitions of the Fourier inverse transform were employed

$$\mathcal{F}^{-1}\{\widehat{f_1}(\gamma)\} = \frac{1}{(2\pi)^{1/2}} \int_{-\infty}^{\infty} \widehat{f_1}(\gamma) \mathrm{e}^{i\gamma x} \, \mathrm{d}\gamma, \tag{A10}$$

$$\mathcal{F}^{-1}\{\widehat{f_1}(\gamma)\widehat{f_2}(\gamma)\} = \frac{f_1(x) * f_2(x)}{(2\pi)^{1/2}}$$

$$= \frac{1}{(2\pi)^{1/2}} \int_{-\infty}^{\infty} f_1(x - \xi) f_2(\xi) \, \mathrm{d}\xi, \tag{A11}$$

where f_1 and f_2 are arbitrary functions of x; and ξ is a dummy integration variable. It should be noted, however, that Euler's formula was employed in the derivation (A9). In view of (A11) and the integral identities found in Gradshteyn and Ryzhik (1980) (Equations 3.724.1 & 2, p. 407), the expression (A9) is simplified as

$$\dot{\overline{\tilde{C}}}(s, x, \omega, \phi) = \frac{\dot{\overline{\tilde{F}}}(s, x, \omega, \phi)}{2\pi D_x} * \left\{ \Psi \exp\left[\frac{Ux}{2D_x} \right] \right\}, \tag{A12}$$

where

$$\Psi = \pi \left(\frac{E}{D_x} + \frac{U^2}{4D_x^2} \right)^{-1/2} \exp\left[-x \left(\frac{E}{D_x} + \frac{U^2}{4D_x^2} \right)^{1/2} \right]. \tag{A13}$$

In view of (A10), (A11), and (A13), the expression (A12) is written as

$$\dot{\tilde{\bar{C}}}(s, x, \omega, \phi) = \int_{-\infty}^{\infty} \dot{\tilde{\bar{F}}}(s, q, \omega, \phi) \, f(s, x - q, \omega, \phi) \, dq, \tag{A14}$$

where

$$f(s, x, \omega, \phi) = \left(\frac{1}{4D_x D_y \, (\omega^2 + S)} \right)^{1/2} \exp\left[\frac{Ux}{2D_x} \right] \times$$

$$\times \exp\left[-x \left((\omega^2 + S) \frac{D_y}{D_x} \right)^{1/2} \right], \tag{A15}$$

$$S = \frac{1}{D_y} \left(\phi^2 D_z + \mathcal{A} + s - \frac{\mathcal{B}}{s + \mathcal{H}} + \frac{U^2}{4D_x} \right), \tag{A16}$$

and q is a dummy integration variable.

In view of (A10), (A11), and (A15), the Fourier inverse transformation of (A14) with respect to ω is given by

$$\tilde{\bar{C}}(s, x, y, \phi)$$

$$= \left(\frac{1}{16\pi^2 D_x D_y} \right)^{1/2} \int_{-\infty}^{\infty} \exp\left[\frac{U(x - q)}{2D_x} \right] \times \tag{A17}$$

$$\times \left\{ \tilde{\bar{F}}(s, q, y, \phi) * \left[\int_{-\infty}^{\infty} \Phi \cos(\omega y) \, d\omega + \int_{-\infty}^{\infty} i \Phi \sin(\omega y) d\omega \right] \right\} dq,$$

where

$$\Phi = \left(\frac{1}{\omega^2 + S} \right)^{1/2} \exp\left[-(x - q) \left((\omega^2 + S) \frac{D_y}{D_x} \right)^{1/2} \right], \tag{A18}$$

and Euler's formula was employed in the derivation of (A17). It should be noted that Φ as well as $\cos(\omega y)$ are even functions of ω, whereas $\sin(\omega y)$ is an odd function of ω. Therefore, the trigonometric integrals are evaluated as follows

$$\int_{-\infty}^{\infty} \Phi \cos(\omega y) \, d\omega = 2 \int_{0}^{\infty} \Phi \cos(\omega y) \, d\omega$$

$$= 2K_0 \left[S^{1/2} \left(y^2 + \frac{(x - q)^2 D_y}{D_x} \right)^{1/2} \right], \tag{A19}$$

$$\int_{-\infty}^{\infty} i\Phi \sin(\omega y) \, d\omega = 0, \tag{A20}$$

where K_0 is the modified Bessel function of the second kind of zeroth order; and the integral identity found in Gradshteyn and Ryzhik (1980) (Equation 3.961.2, p. 498) was utilized in (A19). In view of (A19), (A20) and application of the convolution theorem, (A17) reduces to

$$\tilde{C}(s, x, y, \phi) = \int_{-\infty}^{\infty} \int_{-\infty}^{\infty} \tilde{F}(s, q, v, \phi) \, g(s, x - q, y - v, \phi) \, dv \, dq, \tag{A21}$$

where

$$g(s, x, y, \phi) = \left(\frac{1}{4\pi^2 D_x D_y}\right)^{1/2} \exp\left[\frac{Ux}{2D_x}\right] K_0\left[s^{1/2}\left(y^2 + \frac{x^2 D_y}{D_x}\right)^{1/2}\right], \tag{A22}$$

and v is a dummy integration variable.

In view of (A10), (A11), (A16) and (A22), the Fourier inverse transformation of (A21) with respect to ϕ is given by

$$\tilde{C}(s, x, y, z)$$

$$= \left(\frac{1}{16\pi^4 D_x D_y}\right)^{1/2} \int_{-\infty}^{\infty} \int_{-\infty}^{\infty} \exp\left[\frac{U(x-q)}{2D_x}\right] \times$$

$$\times \left\{ \tilde{F}(s, q, v, z) * \left[\int_{-\infty}^{\infty} K_0[\mathcal{N}(s, x-q, y-v, \phi)] \cos(\phi z) \, d\phi + \right. \right.$$

$$\left. \left. + \int_{-\infty}^{\infty} K_0[\mathcal{N}(s, x-q, y-v, \phi)] i \sin(\phi z) \, d\phi \right] \right\} dv \, dq, \tag{A23}$$

where the following substitutions were employed

$$\mathcal{N}(s, x, y, \phi) = [\phi^2 + \mathcal{N}_1(s)]^{1/2} \mathcal{N}_2(x, y), \tag{A24}$$

$$\mathcal{N}_1(s) = \frac{1}{D_z}\left(\mathcal{A} + s - \frac{\mathcal{B}}{s + \mathcal{H}} + \frac{U^2}{4D_x}\right), \tag{A25}$$

$$\mathcal{N}_2(x, y) = \left(\frac{y^2 D_z}{D_y} + \frac{x^2 D_z}{D_x}\right)^{1/2}. \tag{A26}$$

It should be noted that $\mathcal{N}$ and $\cos(\phi z)$ are even functions of ϕ, whereas $\sin(\phi z)$ is an odd function of ϕ. Therefore,

$$\int_{-\infty}^{\infty} K_0[\mathcal{N}(s, x, y, \phi)] \cos(\phi z) \, d\phi$$

$$= 2 \int_0^{\infty} K_0[\mathcal{N}(s, x, y, \phi)] \cos(\phi z) \, d\phi$$

$$= \left(\frac{\pi^2}{\mathcal{N}_2^2 + z^2} \right)^{1/2} \exp\left[-\mathcal{N}_1^{1/2} (\mathcal{N}_2^2 + z^2)^{1/2} \right], \tag{A27}$$

$$\int_{-\infty}^{\infty} i K_0[\mathcal{N}(s, x, y, \phi)] \sin(\phi z) \, d\phi = 0, \tag{A28}$$

where the integral identity found in Gradshteyn and Ryzhik (1980) (Equation 6.677.5, p. 736) was employed in (A27). In view of (A27), (A28), and application of the convolution theorem, (A23) reduces to

$$\widetilde{C}(s, x, y, z) = \int_{-\infty}^{\infty} \int_{-\infty}^{\infty} \int_{-\infty}^{\infty} \widetilde{F}(s, q, v, p) \times$$

$$\times h(s, x - q, y - v, z - p) \, dp \, dv \, dq, \tag{A29}$$

where

$$h(s, x, y, z) = h_1(s, x, y, z) \, h_2(x, y, z), \tag{A30}$$

$$h_1(s, x, y, z) = \exp[-\mathcal{N}_1^{1/2} (\mathcal{N}_2^2 + z^2)^{1/2}], \tag{A31}$$

$$h_2(x, y, z) = \left[\frac{1}{16\pi^2 D_x D_y (\mathcal{N}_2^2 + z^2)} \right]^{1/2} \exp\left[\frac{Ux}{2D_x} \right]. \tag{A32}$$

Furthermore, for mathematical convenience, let

$$h_1 = \frac{\mathcal{H} h_1}{s + \mathcal{H}} + \frac{s h_1}{s + \mathcal{H}}. \tag{A33}$$

The inverse Laplace transform of (A29) with respect to s can be found by employing the following relationship

$$\mathcal{L}^{-1} \left\{ \frac{1}{s + \mathcal{H}} \widetilde{f}_0 \left(s + \mathcal{H} - \frac{a}{s + \mathcal{H}} \right) \right\}$$

$$= e^{-\mathcal{H}t} \int_0^t I_0 \left[2 \left(a\zeta(t - \zeta) \right)^{1/2} \right] f_0(\zeta) \, d\zeta, \tag{A34}$$

where $\mathcal{L}^{-1}$ is the Laplace inverse operator; $\widetilde{f}_0(s)$ is the Laplace transform of the arbitrary function $f_0(t)$; and a is an arbitrary constant. Equation (A34) was obtained

from the inverse Laplace transform pair reported by Lapidus and Amundson (1952) modified by direct application of the Bessel function relationship $I_0[\eta] = J_0[i\eta]$, where J_0 is the Bessel function of the first kind of zeroth order, and η is an arbitrary argument (Abramowitz and Stegun, 1972, Equation 9.6.3, p. 375). In view of (A25), (A26), and (A31), $\widetilde{f_0}(s)$ is assumed to be of the following form

$$\widetilde{f_0}(s) = \exp\left[-a_1(s + a_2)^{1/2}\right], \tag{A35}$$

where a_1 and a_2 are arbitrary constants. Furthermore, the inverse Laplace transform of $\widetilde{f_0}(s)$ is (Roberts and Kaufman, 1966)

$$f_0(t) = \mathcal{L}^{-1}\left\{\exp\left[-a_1(s + a_2)^{1/2}\right]\right\} = \frac{a_1}{(4\pi t^3)^{1/2}} \exp\left[\frac{-a_1^2}{4t} - a_2 t\right]. \tag{A36}$$

Equation (A35) can also be used to express h_1 as

$$h_1 = \widetilde{f_0}\left(s + \mathcal{H} - \frac{a}{s + \mathcal{H}}\right)$$

$$= \exp\left[-\frac{a_1}{(s + \mathcal{H})^{1/2}}\{s^2 + s(2\mathcal{H} + a_2) + \mathcal{H}(\mathcal{H} + a_2) - a\}^{1/2}\right]. \tag{A37}$$

Substitution of (A25) into (A31) yields

$$h_1 = \exp\left[-\left(\frac{\mathcal{N}_2^2 + z^2}{D_z(s + \mathcal{H})}\right)^{1/2} \times\right.$$

$$\left. \times \left\{s^2 + s\left(\mathcal{H} + \mathcal{A} + \frac{U^2}{4D_x}\right) + \mathcal{H}\left(\mathcal{A} + \frac{U^2}{4D_x}\right) - \mathcal{B}\right\}^{1/2}\right]. \tag{A38}$$

The unknown constants a, a_1, and a_2 are obtained by simple comparison of (A37) and (A38)

$$a = \mathcal{B}, \tag{A39}$$

$$a_1 = \left(\frac{\mathcal{N}_2^2 + z^2}{D_z}\right)^{1/2}, \tag{A40}$$

$$a_2 = \mathcal{A} + \frac{U^2}{4D_x} - \mathcal{H}. \tag{A41}$$

In view of (A34), (A36), and (A39)–(A41), the following inverse Laplace transform is derived

$$\mathcal{L}^{-1}\left\{\frac{h_1}{s + \mathcal{H}}\right\} = \mathcal{P}(t, x, y, z), \tag{A42}$$

where

$$
\mathcal{P}(t, x, y, z) = e^{-\mathcal{H}t} \int_0^t I_0\Big[2\big(\mathcal{B}\zeta(t-\zeta)\big)^{1/2}\Big]\left(\frac{\mathcal{N}_2^2 + z^2}{4\pi D_z \zeta^3}\right)^{1/2} \times
$$

$$
\times \exp\left[-\frac{\mathcal{N}_2^2 + z^2}{4 D_z \zeta} - \zeta\left(\mathcal{A} + \frac{U^2}{4D_x} - \mathcal{H}\right)\right] d\zeta. \tag{A43}
$$

Furthermore, the Laplace transform of a first-order derivative found in Kreyszig (1993) (Equation 6.2, p. 317), together with $\mathcal{P}(0, x, y, z) = 0$ suggests that

$$
\mathcal{L}^{-1}\left\{\frac{s h_1}{s + \mathcal{H}}\right\} = \mathcal{L}^{-1}\left\{s\widetilde{\mathcal{P}}(s, x, y, z)\right\} = \frac{\partial \mathcal{P}(t, x, y, z)}{\partial t}. \tag{A44}
$$

In view of (A33), (A42) and (A44), the inverse Laplace transformation of (A29) is given by

$$
C(t, x, y, z)
$$

$$
= \int_0^t \int_{-\infty}^{\infty} \int_{-\infty}^{\infty} \int_{-\infty}^{\infty} F(t-\tau, q, v, p)\, h_2(x - q, y - v, z - p) \times
$$

$$
\times \Big[\mathcal{H}\mathcal{P}(\tau, x - q, y - v, z - p) \;+
$$

$$
+ \frac{d\mathcal{P}(\tau, x - q, y - v, z - p)}{d\tau}\Big]\, dp\, dv\, dq\, d\tau, \tag{A45}
$$

where the following inverse Laplace transform relationship was employed

$$
\mathcal{L}^{-1}\left\{\widetilde{f}_1(s)\widetilde{f}_2(s)\right\} = f_1(t) * f_2(t) = \int_0^t f_1(t - \tau) f_2(\tau)\, d\tau. \tag{A46}
$$

Backsubstituting (A26), (A32) and (A43) into (A45) yields the desired generalized analytical solution (12)–(14).

Acknowledgements

References

Abramowitz, M. and Stegun, I. A.: 1972, *Handbook of Mathematical Functions*, Dover, New York.
Armon, R. and Kott, Y.: 1994, The health dimension of groundwater contamination, in: U. Zoller (ed.), *Groundwater Contamination and Control,* Marcel Dekker, New York, pp. 71–85.

Bales, R. C., Li, S., Maguire, K. M., Yahya, M. T., Gerba, C. P. and Harvey, R. W.: 1995, Virus and bacteria transport in a sandy aquifer, Cape Cod, MA, *Ground Water* **33**(4), 653–661.

Bales, R. C., Li, S., Yeh, T. -C. J., Lenczewski, M. E. and Gerba, C. P.: 1997, Bactriophage and microsphere transport in saturated porous media: Forced-gradient experiment at Borden, Ontario, *Water Resour. Res.* **33**(4), 639–648.

Batu, V.: 1989, A generalized two-dimensional analytical solution for hydrodynamic dispersion in bounded media with the first-type boundary condition at the source, *Water Resour. Res.* **25**(6), 1125–1132.

Batu, V.: 1993, A generalized two-dimensional analytical solute transport model in bounded media for flux-type finite multiple sources, *Water Resour. Res.* **29**(8), 1125–1132.

Batu, V. and van Genuchten, M. T.: 1990, First- and third-type boundary conditions in two-dimensional solute transport modeling, *Water Resour. Res.* **26**(2), 339–350.

Bellin, A., Rinaldo, A., Bosma, W. J. P., van der Zee, S.E.A.T.M. and Rubin, Y.: 1993, Linear equilibruim adsorbing solute transport in physically and chemically heterogeneous porous formations, 1, Analytical solutions, *Water Resour. Res.* **29**(12), 4019–4030.

Berg, G.: 1977, Viruses in the environment: Criteria for risk, in: B. P. Sagik and C. A. Sorber (eds.), *Risk Assessment and Health Effects of Municipal Wastewater and Sludges*, Proceedings, Univ. Texas, San Antonio, pp. 216–229.

Birgersson, L. and Neretnieks, I.: 1982, Diffusion in the matrix of granitic rock field test in the Stripa mine, Part 1, SKBF/KBS Teknish Rapport, 82-08, Royal Inst. Technol., Stockholm, Sweden.

Brock, T. D. and Madigan, M. T.: 1991, *Biology of Microorganisms*, 6th edn, Prentice-Hall, Englewood Cliffs, p. 874.

Buddemeier, R. W. and Hunt, J. R.: 1988, Transport of colloidal contaminants in groundwater radionuclide migration at the Nevada test site, *Applied Geochem.* **3**, 535–548.

Chrysikopoulos, C. V.: 1995, Three-dimensional analytical models of contaminant transport from nonaqueous phase liquid pool dissolution in saturated subsurface formations, *Water Resour. Res.* **31**(4), 1137–1145.

Chrysikopoulos, C. V. and Sim, Y.: 1996, One-dimensional virus transport in homogeneous porous media with time dependent distribution coefficient, *J. Hydrol.* **185**, 199–219.

Chrysikopoulos, C. V., Voudrias, E. A. and Fyrillas, M. M.: 1994, Modeling of contaminant transport resulting from dissolution of nonaqueous phase liquid pools in saturated porous media, *Transport in Porous Media* **16**(2), 125–145.

Elimelech, M., Gregory, J., Jia, X. and Williams, R. A.: 1995, *Particle Deposition and Aggregation: Measurement, Modeling and Simulation,* Butterworth-Heinemann, Oxford, Great Britain.

Gerba, C. P. and Keswick, B. H.: 1981, Survival and transport of enteric bacteria and viruses in groundwater, *Stud. Environ. Sci.* **17**, 511–515.

Goltz, M. N. and Roberts, P. V.: 1986, Three-dimensional solutions for solute transport in an infinite medium with mobile and immobile zones, *Water Resour. Res.* **22**(7), 1139–1148.

Gradshteyn, I. S. and Ryzhik, I. M.: 1980, *Table of Integral, Series, and Products*, Academic Press, New York.

Greenberg, M. D.: 1978, *Foundations of Applied Mathematics*, Prentice-Hall, Englewood Cliffs.

Grosser, P. W.: 1984, A one-dimensional mathematical model of virus transport, Paper presented at the Second International Conference on Ground-Water Quality Research, Tulsa, OK., Mar. pp. 26–29.

Haridas, A.: 1984, A mathematical model of microbial transport in porous media, PhD Dissertation, Univ. of Delaware.

Harvey, R. W. and Garabedian, S. P.: 1991, Use of colloid filtration theory in modeling movement of bacteria through a contaminated sandy aquifer, *Environ. Sci. Technol.* **25**(1), 178–185.

Hassani, S.: 1991, *Foundations of Mathematical Physics*, Allyn and Bacon, Boston.

Hunt, B.: 1978, Dispersive Sources in uniform groundwater flow, *J. Hydraul. Div. Am. Soc. Civ. Eng.* **104**(HY1), 75–85.

IMSL: 1991, IMSL MATH/LIBRARY user's manual, ver. 2.0, IMSL, Houston.

Kahaner, D., Moler, C. and Nash, S.: 1989, *Numerical Methods and Software*, Prentice-Hall, Englewood Cliffs.

Keswick, B. H. and Gerba, C. P.: 1980, Viruses in groundwater, *Environ. Sci. Technol.* **14**, 1290–1297.

Kreyszig, E.: 1993, *Advanced Engineering Mathematics*, 7th edn, Wiley, New York.

Lapidus, L. and Amundson, N. R.: 1952, Mathematics of adsorption in beds, VI. The effect of longitudinal diffusion in ion exchange and chromatographic columns, *J. Phys. Chem.* **56**, 984–988.

Leij, F. J. and Dane, J. H.: 1990, Analytical solutions of the one-dimensioal advection equation and two- or three-dimensional dispersion equation, *Water Resour. Res.* **26**(7), 1475–1482.

Leij, F. J., Skaggs, T. H. and van Genuchten, M. Th.: 1991, Analytical solutions for solute transport in three-dimensional semi-infinite porous media, *Water Resour. Res.* **27**(10), 2719–2733.

Leij, F. J., Toride, N. and van Genuchten, M. Th.: 1993, Analytical solutions for nonequilibrium solute transport in three-dimensional porous media, *J. Hydrol.* **151**, 193–228.

Li, S.: 1993, Modeling biocolloid transport in saturated porous media, PhD Dissertation, Univ. of Arzona, Tucson.

Matthess, G. and Pekdeger, A.: 1981, Concepts of a survival and transport model of pathogenic bacteria and viruses in groundwater, *Sci. Tot. Environ.* **21**, 149–159.

Mitchell, J. K.: 1976, *Fundamentals of Soil Behavior*, Wiley, New York.

Park, N., Blanford, T. N. and Huyakorn, P. S.: 1992, VIRALT: *A Modular Semi-Analytical and Numerical Model for Simulating Viral Transport in Ground Water*, International Ground Water Modeling Center, Colorado School of Mines, Golden, CO.

Penrod, S. L.: 1995, The deposition kinetics of Bacteriophage MS2 and λ, Master Thesis, Univ. of California, Irvine, CA.

Roberts, G. E. and Kaufman, H.: 1966, *Table of Laplace Transforms*, W. B. Saunders, Philadelphia, PA.

Sim, Y. and Chrysikopoulos, C. V.: 1995, Analytical models for one-dimensional virus transport in saturated porous media, *Water Resour. Res.* **31**(5), 1429–1437. (Correction: *Water Resour. Res.* **32**(5), p. 1473, 1996.)

Sim, Y. and Chrysikopoulos, C. V.: 1996a, One–dimensional virus transport in porous media with time dependent inactivation rate coefficients, *Water Resour. Res.* **32**(8), 2607–2611.

Sim, Y. and Chrysikopoulos, C. V.: 1996b, Parameter sensitivity of macroscopic virus transport in porous media with temporally variable inactivation, in: H. J. Morel–Seytoux (ed.), *Sixteenth Annual American Geophysical Union Hydrology Days*, Fort Collins, CO., pp. 455–466.

Stumm, W.: 1977, Chemical interaction in particle separation, *Environ. Sci. Technol.* **11**, 1066–1070.

Taylor, D. H. and Bosmann, H. B.: 1981, The electrokinetic properties of reovirus type 3: Electrophoretic mobility and zeta potential in dilute electrolytes, *J. Colloid Interface Sci.* **83**, 153–162.

Tim, U. S. and Mostaghimi, S.: 1991, Model for predicting virus movement through soils, *Ground Water* **29**(2), 251–259.

van Dujin, C. J. and van der Zee, S.E.A.T.M.: 1986, Solute transport parallel to an separating two different porous materials, *Water Resour. Res.* **22**(13), 1779–1789.

Vilker, V. L., Frommhagen, L. H., Kamda, R. and Sundaram, S.: 1978, Application of ion exchange/adsorption models to virus transport in percolating beds, *AIChE Symp. Ser.* **74**(178), 84–92.

Vilker, V. L.: 1981, Simulating virus movement in soils, in: I. K. Iskandar (ed.), *Modeling Waste Renovation; Land Treatment*, Wiley, New York, pp. 223–253.

Yates, M. V. and Yates, S. R.: 1988, Modeling microbial fate in the subsurface environment, *Crit. Rev. Environ. Control* **17**(4), 307–344.

Yates, M. V. and Ouyang, Y.: 1992, VIRTUS: A model of virus transport in unsaturated soils, *Appl. Environ. Microb.* **58**(5), 1609–1616.

Zelikson, R.: 1994, Microorganisms and viruses in groundwater, in: U. Zoller (ed.), *Groundwater Contamination and Control,* Marcel Dekker, New York, pp. 425–436.